

Automatic Exudate Detection from Retinal Fundus Images in Diabetic Retinopathy

Manisha L. Jadhav^{1*}, Shrikant J. Honade², Anil L. Wanare³, Vijay M. Sardar⁴

^{1*}Assistant professor, Department of E&TC Engineering, MET's Institute of Engineering, Nasik, (M.S.) India. manishas_ioe@bkc.met.edu

² Asso.Professor & HoD, Department of Electronics Engg (VLSI D & T), Chh. Shahu College of Engineering, Sambhajinagar,

Dr. Babasaheb Ambedkar Technological University, Lonere (M.S.) India. sjhonadeamt@gmail.com

³ Professor, E&TC Engg Dept, Bhivarabai Sawant Institute of Technology and Research, Savitribai Phule Pune University, Pune, (M.S.)

India. anillaxman369@gmail.com

⁴ Associate Professor, Department of E&TC Engineering, Jayawantrao Sawant College of Engineering, Savitribai Phule Pune University Pune, (M.S.) India. vijaysarda@jspmjscoe.edu.in

How to cite this article: Manisha L. Jadhav, Shrikant J. Honade, Anil L. Wanare, Vijay M. Sardar (2024) Automatic Exudate Detection from Retinal Fundus Images in Diabetic Retinopathy. *Library Progress International*, 44(3), 2662-2671.

ABSTRACT

Diabetes results in diabetic retinopathy, which occurs due to a change in the vasculature structure. Diabetic abnormalities such as microaneurysms, haemorrhages, and "exudates" describe the stage of diabetic retinopathy. Early-stage detection gains prime importance to avoid permanent sight loss. Exudates are one of the most noticeable signs of diabetic retinopathy. This work presents the automatic and non-invasive approach to detect exudates using requisitely adjusted morphological operators. The use of Standard deviation of histogram equalized image after optic disc detection and deletion is the work's key contribution. The standard deviation offers the tendency of distributing the favourable exudate pixels towards the mean value. The proposed method is implemented on the "IDRiD (Indian Diabetic Retinopathy Image Dataset)". The detected exudates are compared with provided ground-truths reported accuracy of 99.13%. The outcomes prove its effectiveness of the proposed method and can aid ophthalmologists in diagnosis.

Keywords: Diabetic Retinopathy (DR), Exudates, Morphological operations, Optic Disc, Fundus image.

Introduction

According to the World Health Organization (WHO), elevated blood sugar levels induce metabolic disorders resulting in diabetes. Thus, long-term diabetes leads to neuropathy and retinopathy. People having chronic diabetes may suffer from heart disease, obesity, cataracts etc. [1]. There is a steady rise in diabetic patients worldwide. The rate of diabetic patients is higher in developing countries than in developed countries [2]. As per WHO, the estimated cases of adults having diabetes were 422 million in 2014. The International Diabetes Federation estimates that there are 1.1 million children and adults who have type 1 diabetes. If precaution is ignored, this may lead to 629 million diabetic patients by 2045 [3]. Long-term diabetes causes preventable damage to the eye. However, loss can be avoided with periodic eye tests followed by appropriate treatment. The eye examination is based on retina images obtained with a fundus camera, which represent bright and dark lesions in the retina. [4].

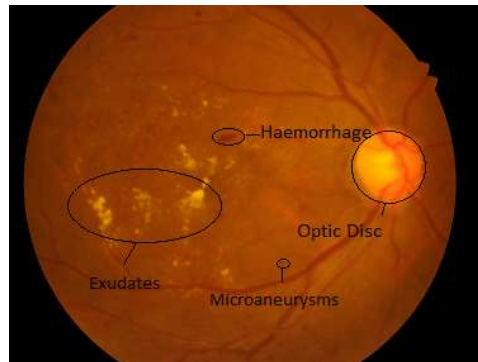


Fig.1.Fundus image with retinal lesions.

The microaneurysms and haemorrhages are dark lesions, whereas bright lesions are exudates. The identification of exudates aids when evaluating macular edema and diabetic retinopathy. [5]. Figure 1 depicts retinal fundus images with optic disc and different lesions.

The exudates appear white or yellowish to humans and have a variety of forms, sizes, and locations. They usually appear in a cluster form, or sometimes it seems single. The exudates are formed due to the swelling of tiny vessels, causing the leakage of protein-rich fluids into a retinal nerve. The fluid built up plasma taking yellowish plaque or dots that shows an attraction toward macula [6]. The exudates may take the form of wax-like plaque, a ring, or appear as a cluster of tiny deposits [7].

This research work deals with exudates detection for DR. The approach with optimized morphological operations has been introduced. The following is how the paper is organized: Section 2 examined the literature on the detection of exudates. Section 3 explains the pre-processing of retinal images, which is followed by optic disc detection and deletion utilizing thresholding and morphological reconstruction. Further, the exudates are caught from the optic disc eliminated image by calculating standard deviation. Sections 4 and 5 cover the experimental findings and the discussion. Section 6 presents the experimentally derived result.

There are various approaches available and presented in the literature from different authors for accurate diagnosis based on segmentation of DR lesions.

A back-propagation neural network technique to detecting diabetic retinopathy is presented in [5]. The work is carried out on grey-level images to detect the exudates. This algorithm was not suitable for low contrast images. The detection rate achieved for vessels, exudates and haemorrhages are 91.7%, 93.1%, and 73.8%, respectively.

The domain knowledge about the blood vessels by using a vessel recognition algorithm to detect vessels and a median filter of size 20×20 was used in [8] to suppress the vessels and other artefacts. Further, the vessels were separated from their background using dynamic clustering and the hard exudates were detected from 543 retinal images. The sensitivity and specificity achieved was 100% and 74%, respectively. An innovative move towards optic disc detection has been put forth in [9] using intensity variation criteria. Principal component analysis (PCA) of an image was used to train a multilayer perceptron neural network to recognize blood vessels. The edge detection of the first component of PCA was done. The correlation was matched with the property of fovea. The approach to detect shape of exudates have been proposed in [10], the watershed transformation and morphological operations were used to segment optic disc with a sensitivity of about 92.8% and 92.4% was a mean predictive value. The standardization of the colour [11] of each retinal image is done, as it varies from person to person. After that, the image contrast at a local level was enhanced to make the segmentation easier. Neural networks and fuzzy C-means clustering were employed, to extract features. An improved Fuzzy C-means in LUV colour space is proposed in [12] to segment bright lesions. The classification of actual bright lesions from non- lesions was done using SVM classifier. Classification sensitivity and specificity were 97% and 96%, respectively. [13] describes a unique approach for fine segmentation of exudates using Fuzzy C-means clustering and coarse segmentation utilizing standard deviation. The results were validated using hand-picked ophthalmologist ground-truths, with sensitivity and specificity of 86% and 99%, respectively. Fisher's discriminant analysis is used to classify exudates based on colour features in [14]. They have used 58 images with variation, in contrast, colour and quality, obtaining a sensitivity of 88% for exudates detection. A fuzzy interference system is developed to classify exudates and non-exudates [15]. They reported 93.84% accuracy, 91.11% sensitivity, and 100% specificity for detecting exudates using a morphological technique. A system for grading the hard exudates using a polar coordinate system centered at the fovea [16]. The region growing was combined with edge detection for finding local threshold. The sensitivity of exudates detection achieved was 93.2% based on clinician hand-drawn ground-truths. A Gaussian mixture model classifier [17] to classify the exudates from detected lesions. The filter bank with adaptive thresholding were used for exudates detection and the optic disc was eliminated. The colour, shape and statistical properties of exudates were used for feature extraction. The sensitivity and specificity achieved for the STARE dataset were 97.72% and 96.15%, respectively.

A novel approach is proposed in [18] to eliminate the image's noise to reduce the false positives by enhancing the accuracy. This was accomplished by combining two separate methods based on threshold edge detection. A mathematical modeling approach is put forth in [19] to emphasize the bright intensity pixels to detect optic disc and

exudates efficiently. The classification of healthy and DR images is made based on detected exudates. They have achieved a classification accuracy of more than 98%. A novel approach is defined by combining a morphological approach with intensity thresholding for detecting small exudates while removing all false positives in [20]. The reflection noise and blood vessels were removed with the combined approach to make the detection more accurate. A novel method is presented in [21] for selecting efficient features from the detected exudates and haemorrhages using a voting machine. They have used statistical, textural and fractal characteristics of corresponding areas in the fundus image. The efficiency of selected features was calculated by using the gliding box and fixed box segmentation technique. The sensitivity and specificity of 95.14% and 94.52% were achieved for exudates detection respectively. A morphological compact tree-based detection of exudates is put forth in [22]. By using blobbing technique, all connected pixels counted as a single blob. The area filter was applied to filter blobs with higher areas. The medium blobs were again pre-processed such that firm boundaries were eliminated and supposed candidates were extracted. All blobs were further applied to a compact morphological tree to remove the non-exudates region by keeping a manual threshold for each image.

A histogram thresholding technique for detecting exudates after detecting the optic disc by localizing its center and eliminating it is presented in [23]. Thus in the absence of an optic disc, the exudates were easily seen being yellowish-white in intensity. The algorithm was tested with STARE, DRIVE and DIARETDB1 datasets and with a local dataset with 325 images. It achieved an accuracy of 93%, 100%, 96%, and 97%, respectively. It is proposed to use dynamic thresholding in conjunction with global thresholding based on FCM in [24] to detect hard exudates followed by texture features from candidate regions. An SVM classifier did the classification. In [25], an image set that corresponds to hard exudates is prepared, as well as an image set that does not. This set of images is used to build the convolutional network. The convolutional network is put to the test further for sensitivity and specificity. Transfer learning to extract the features using CNN models is performed in [26]; additionally, the exudates from fused features from completely linked layers are classified using the softmax classifier.

Numerous work has been carried out on exudates detection in literature. Some of the work has been implemented on images after dilating the pupil to make the retinal features more clearly detectable. Based on previous work mentioned in the literature, high-quality images have been used to carry out experimentation. The low-contrast images are blurred and with non-uniform illumination, so most of the algorithms may not work.

The present work has been implemented on retinal images obtained with a fundus camera. The paper presents a morphological approach for exudates detection in retinal images from the IDRiD dataset, the first dataset representative of the Indian population. The work's principal contribution is the use of standard deviation of histogram equalized image after optic disc detection and deletion. The standard deviation offers the tendency of distributing the favorable exudate pixels towards the mean value. The exudates detected in the center of the retina near the macular region normally define the severity of the disease. The severity increases with an increase in exudates in the centre of retina.

3. Methodology

The proposed method for identifying exudates is provided, discussed, and illustrated below in figure 2. The IDRiD dataset [27], which consists of 81 images with exudates ground facts, was employed in the research work for implementation. The resolution of images is 4288×2848.

3.1 Pre-processing

The fundus image captured by a camera is RGB image; the green plane provides a good contrast image as compared to a red and blue plane. So the green plane is passed through the median filter of 3×3 size for removal of noise [28].

To map the pixels in the local neighborhood, the “contrast-limited adaptive histogram equalization (CLAHE)” is applied to the denoised image. The contrast of each tiny section is increased, and the tiny pieces are finally combined via bilinear interpolation.

As a result, the synthetically induced boundaries are removed, and over-amplification is minimized by limiting contrast. [29].

The CLAHE operation applied on the green channel denoised image is given in eq.1.

$$f_h = CLAHE(f_g) \dots \quad (1)$$

f_g - denoised green channel image, f_h - CLAHE image, The clip limit of 0.009 is empirically chosen here.

After the CLAHE operation, the enhanced image shows the bright pixels with high intensity, such as optic disc, exudates, and blood vessels in the centre of the optic disc.

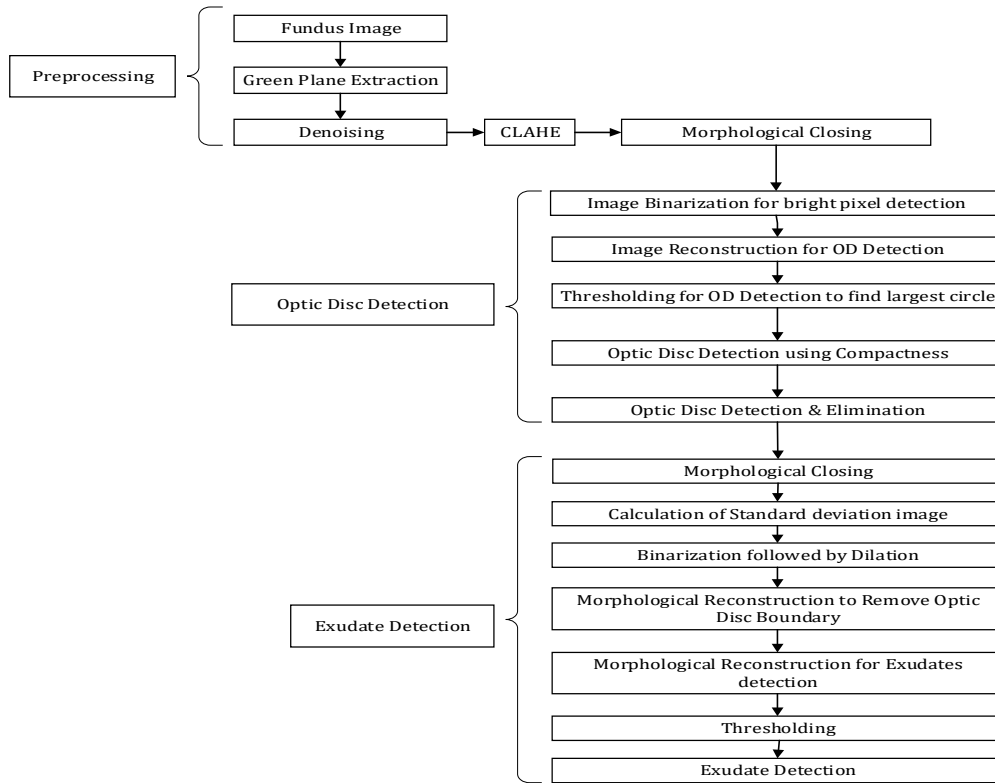


Fig. 2. Schematic representation of the proposed exudates detection system.

3.2 Optic Disc Detection and Elimination

As the blood vessels appear with high contrast in enhanced image, the pre-processed image is passed through the morphological closing operation. The closing operation removes the vessels from the retinal image.

$$f_{o1} = (f_h \oplus s1) \ominus s1 \quad \dots \quad (2)$$

Where $s1$ - Structuring element. The structuring element is chosen to be disc-shaped with various radii such as 4, 5 and 6. The accuracy and specificity results are significantly high for the size 5.

The binarization operation is applied on a morphologically closed image with the threshold value T_{h1} of 0.72. The binarized image consists of the maximum part of optic disc. It is superimposed on the CLAHE image after inversion, as shown in figure 3(d). To encompass all pixels in the optic disc region, the dilation process is followed by morphological reconstruction [30]. The marked objects from the image are extracted without changing their shape and size.

$$f_{o2} = R[s_2 \oplus (f_h - T_{h1}(f_{o1}))] \quad \dots \quad (3)$$

s_2 - disc type structuring element of radius 10. R – Morphological reconstruction

Morphologically reconstructed (f_{o2}) image is subtracted from the CLAHE image. Further, it is thresholded by T_{h2} , as given in equation 4. The threshold value T_{h2} varies based on image intensities by using Otsu’s algorithm [31]. In Otsu’s thresholding approach, the threshold is chosen to minimise the interclass variation in thresholded black and white pixels.

$$f_{o3} = T_{h2}(f_h - f_{o2}) \dots \quad (4)$$

Where T_{h2} is a threshold value, f_h - CLAHE image, f_{o2} – Reconstructed image, f_{o3} - thresholded image

In the thresholded image f_{o3} the brighter portion, such as optic disc and exudates, are apparent while removing the other intensities. The optic disc is typically the greatest portion of the retinal image., but exudates may appear in a larger area in some exceptional cases. To accurately detect the optic disc, the most circular shape must be calculated by calculating compactness. Compactness is the ratio of the object area to the area of the circle with the same perimeter. The maximum

value of compactness is 1. So it is applied to all brighter objects present in the reconstructed image. The maximum value of compactness gives a more circular part, which can be detected as an optic disc [Sinthanayothin et al., 1999]. The compactness is given by the following equation 5.

$$C = \frac{4\pi \times \text{Total no. of pixels in the region}}{(\text{no. of boundary pixels})^2} \dots (5)$$

The largest area in a circular shape f_{o_4} is calculated using the above equation and further. The dilation operation with disc-type structuring element with radius 20 is applied to cover all pixels at the optic disc boundary, as shown in equation 6.

$$OD_{detect} = f_{o_4} \oplus s_2 \quad \dots (6)$$

The OD_{detect} is masked from the input image to mask the optic disc.

$$OD_{elim} = f_h - OD_{detect} \quad \dots (7)$$

3.3 Detection of candidates

After masking the optic disc, the exudates being the high-intensity structures in the image are determined by computing the standard deviation image. It is determined from the OD eliminated image OD_{elim} by using the formula given in equation 8.

$$F_{exu} = \frac{1}{I-1} \times \sum_{j \in m(x)} (OD_{elim}(j) - \mu)^2 \quad \dots (8)$$

where,

x - Set of each pixels in the window $m(x)$,

μ - mean of $OD_{elim}(j)$

$j \in m(x)$ - the chosen window of size 3×3 ,

I - number of pixels in window $m(x)$

Following the calculation of the standard deviation image, the thresholding operation with threshold T_{h3} using Otsu's algorithm followed by dilation operation with a disc size of 5 is applied to include all pixels from the region of interest as given in equation 9.

$$F_{exuD} = s_3 \oplus T_{h3}(F_{exu}) \quad \dots (9)$$

F_{exuD} - dilated image after thresholding, F_{exu} - standard deviation image. The resulting image F_{exuD} consist of dilated exudates and the boundary of the eliminated optic disc. The optic disc boundary is removed by morphologically eroding the image with linear structuring element s_4 of appropriate size as shown in equation 10.

$$F_{exuD1} = s_4 \ominus (F_{exuD}) \quad \dots (10)$$

F_{exuD1} - Eroded image after linear thresholding, s_4 - Linear structuring element

Repeated dilations reconstruct the eroded image. F_{exuD} is a dilated image from which the reconstructed image is subtracted. As illustrated in Equation 11,

$$E_x = F_{exuD} - R(F_{exuD1}) \quad \dots (11)$$

$R(F_{exuD1})$ - Reconstructed image

Further, the variation between the resultant image and the CLAHE image is calculated to create a marker image followed by reconstruction by taking the CLAHE image as a mask.

$$I_{Ex} = f_h - E_x \quad \dots (12)$$

$$I_{Ex1} = f_h - R(I_{Ex}) \quad \dots (13)$$

I_{Ex} is the outcome of the difference between the CLAHE image and the morphologically reconstructed image. $I_{Ex1} = T_{h4}(I_{Ex1}) \quad \dots (14)$

The thresholding operation with a threshold of T_{h4} is applied to the final image I_{Ex1} and here T_{h4} is taken as 0.002 empirically for proper detection of exudates and their cluster.

Finally, the ground truth image supplied with the dataset is compared with the binary image of the identified exudates I_{Ex1} . The accuracy, sensitivity, and specificity are determined by computing the true positives, true negatives, false positives, and false negatives.

4. Experimental Results

MATLAB was used to test 81 images from the IDRiD dataset that had exudates ground truths. The algorithm is divided into three steps; The green plane is separated and denoised from the colour fundus image, followed by CLAHE. The morphological closing operation is used to eliminate the blood vessels. The optic disc, which is in the same intensity as that of exudates, is detected and eliminated with Otsu's thresholding followed by morphological reconstruction operation. The standard deviation image is calculated from optic disc eliminated image. Further, by using thresholding and image

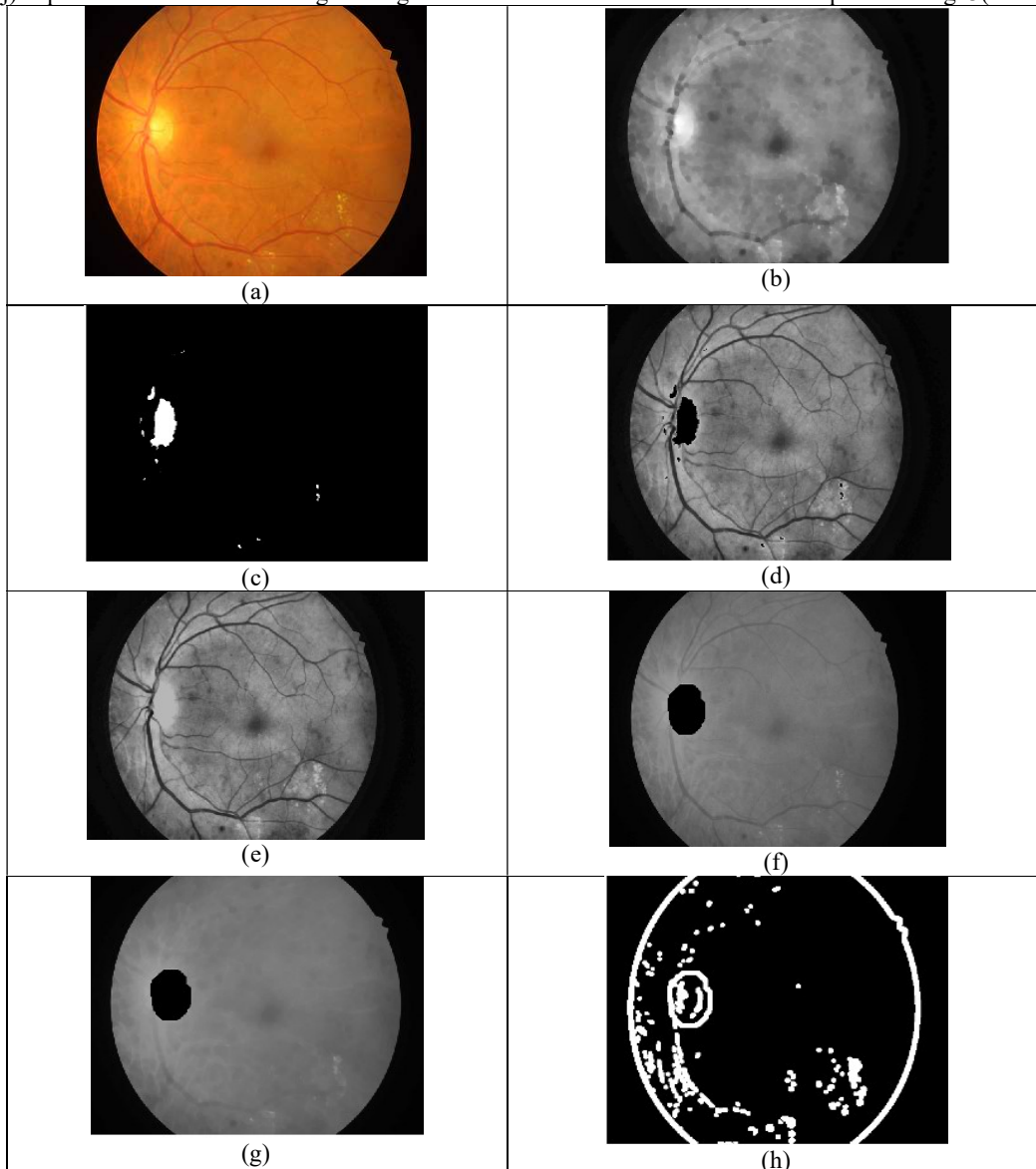
reconstruction operations, the exudates are detected. The processing time for each image was 13 seconds on resized images of size 720×576. Based on the experimentation the true positive (TP), true negative (TN), false positive (FP) and false negative (FN) are calculated by comparing the extracted exudates with ground truths provided with dataset. The performance is evaluated based on sensitivity, specificity and accuracy given as following:

$$sensitivity = \frac{(true\ positive)}{(true\ positive + false\ negative)} \quad (15)$$

$$specificity = \frac{(true\ negative)}{(true\ negative + false\ positive)} \quad (16)$$

$$Accuracy = \frac{(true\ positive + true\ negative)}{(true\ positive + true\ negative + false\ positive + false\ negative)} \quad (17)$$

The colour fundus image from the IDRiD dataset with a resolution of 4288 2848 pixels is shown in Fig. 3 (a). The morphologically closed image of an extracted green plane from the colour fundus image is shown in Fig. 3(b). The closed image is thresholded using Otsu's thresholding as shown in Fig. 3(c). The thresholded image is inverted and applied to the CLAHE image as in Fig. 3(d), which acts as a marker image for image reconstruction. Fig. 3(e) shows a reconstructed image to detect the optic disc. In Fig. 3(f) the optic disc is eliminated after image reconstruction. The optic disc eliminated image is morphologically closed as shown in Fig. 3(g). As illustrated in Fig. 3(h), Otsu's thresholding is applied to the standard deviation image, followed by dilation, and Fig. 3(i) shows the image after removal of optic disc ring from a dilated image. Figure 3(j) depicts the reconstructed image. The ground truths and observed exudates are depicted in Fig. 3(k & l).



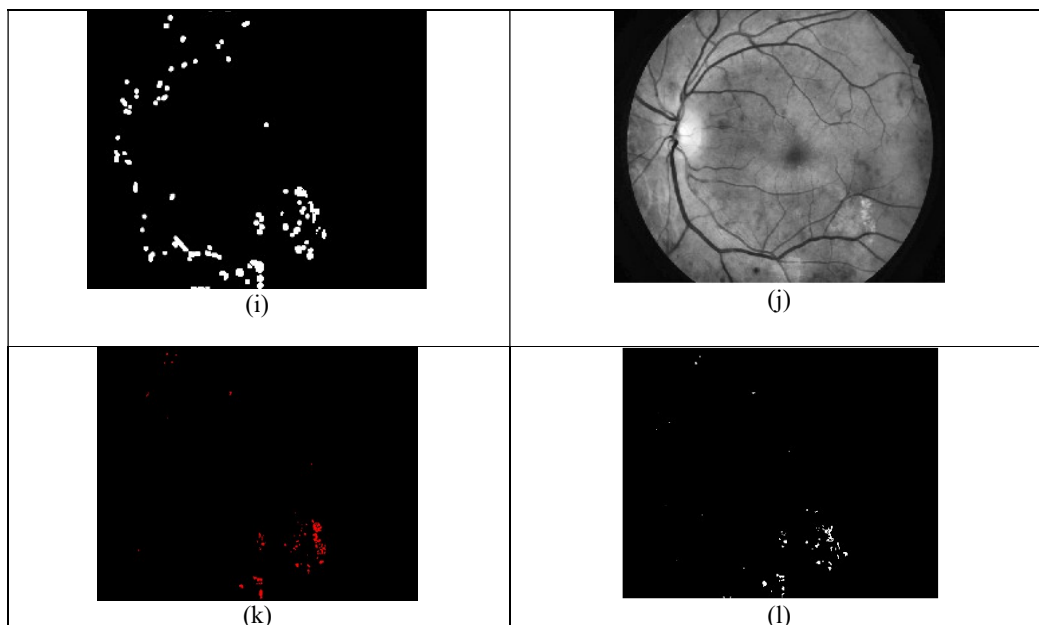


Fig.3 (a) original color fundus image IDRiD dataset with 4288 2848 pixel resolution (b) green plane image after morphological closing (c)binarized image after otsu’s thresholding (d) marker image for image reconstruction (e) morphologically reconstructed image (f) optic disc eliminated from CLAHE image (g) closed image after optic disc elimination (h) Thresholded image after dilation (i) Optic disc boundary eliminated from the thresholded image (j) reconstructed image (k) Exudates ground truth image (l) Detected exudates

The following table shows the accuracy, sensitivity The set of experiments by selecting suitable values of linear structuring elements and different threshold settings is exercised, and maximum sensitivity is achieved 66.28%.and specificity of exudates detection for sample images of the IDRiD dataset.

Table 1. Average Accuracy, sensitivity and specificity of exudates detection for sample images.

Author	Methodology	Database	Accuracy (%)	Sensitivity (%)	Specificity (%)
Wynne Hsu(2001)	Dynamic clustering	Private hospital dataset	--	100	74
		IDRiD	86.15	91.34	75.21
PonnyBala(2012)	fuzzy interference system	Private hospital dataset	93.84	91.11	100
		IDRiD	95.74	74.05	94.01
Umar Aftab(2012)	Colour, shape and statistical properties	STARE Dataset	--	97.72	96.15
		IDRiD	90.23	92.85	94.11
Dan Popescu(2016)	Gliding box and fixed box segmentation	MESSIDOR	--	95.14	94.52
		IDRiD	89.17	91.54	94.85
WilverAuccahuasi(2019)	Convolutional neural network	DIARETDB1	--	92.00	93.00
Muhammad Mateen(2020)	Convolutional neural network	DIARETDB1.	98.43	--	--
Proposed Method	Morphological operations	IDRiD	99.13	66.28	99.15

As compared to datasets presented in literature the proposed methodology shows a bit improvement in specificity and accuracy. However the sensitivity for the IDRiDwhich may be probablylow because of low contrast ratio between exudates and background.

Table 2. Increase in sensitivity by adjusting the intensity threshold.

Structuring element	Threshold(Th ₄)	Sensitivity	Specificity
line, 40,90)	1	53%	36%
line, 50,100)	01	29%	26%
line, 60,100)	02	28%	15%
line,70,110)	04	28%	15%

From the above table maximum increase of 4.75 % is observed in sensitivity, with minor degradation i.e. 0.21% in specificity value. And enhancing sensitivity further is beyond the scope of this methodology. Here, we consider the improved sensitivity i.e. 66.28%.

The proposed method is also applied to private hospital dataset. The live dataset with 91 images is obtained from Navkar Hospital Nasik (Maharashtra, India). The obtained results such as accuracy, sensitivity and specificity are shown in table 3.

Table 3 Average Accuracy, sensitivity and specificity of exudates detection for private hospital dataset.

Total no of images	Accuracy	Sensitivity	Specificity
91	66%	54%	89%

The above results are based on the hand drawn ground-truths by ophthalmologist.

Table 4 Comparison of processing time for different studies in literature using morphological operations.

Sr no.	Author	Database	Methodology	No. of bits for per pixel	Processing time
1	Sopharak (2010)	Private Database	FCM clustering followed by Morphological reconstruction	24	3 minutes
2	Kittipolwisang (2017)	DIARETDB1	Morphology mean shift algorithm followed by morphological operations Segmentation: Two-step (Coarse and fine)	24	1.24 minutes (46 seconds for preprocessing, 31 seconds for candidate extraction and 7 seconds for final exudate detection)
3	Proposed method	IDRiD	Morphological operations	8	13 seconds

The proposed undertaking compared in table 4 w.r.t. the processing time with the similar work is given using morphological operations for extraction of exudates:

The proposed work significantly improves the processing speed. In other mentioned researches by two authors, the colour images processed with 24 bits. However, the proposed work utilized only a green plane image which needs 8 bits per pixel. The saving is considerable w.r.t. number of computations over the entire image. In addition, the proposed work uses images with good contrast compared to work presented by [32], where the images from private hospitals consisting of varying contrast are utilized. It reduces the efforts and hence time to compensate for the diversities in the proposed setup. In the work presented by [32,33], the segmentation process is carried out in two steps namely coarse segmentation followed by fine segmentation of exudates. As the proposed work is intended for the mass detection in medical camp scenario, the segmentation of exudates is carried out by computing a standard deviation image to determine high intensity structures. So comparatively takes much less time.

5. Discussion

The proposed approach presents automatic exudates detection based on morphological operations. The early finding of exudates followed by timely treatment can save eyesight. As the optic disc and exudates have the same intensity, the optic disc is detected and removed effectively. The system can assist the ophthalmologist by detecting the lesions at an earlier stage to a certain extent for reducing their workload. As the number of an ophthalmologist is not sufficient in developing countries, the work presented here can be a tool for the primary diagnosis of retinopathy. The artefact from noise during the image acquisition step causes some incorrect detection of exudates. Specificity measures a test's capacity to provide a negative result for those who do not have exudate pixels in the DR test. (also known as the "true negative" rate). High specificity means the test won't generate many false-positive results. Sensitivity is a measure of how frequently a test produces a positive result for ill persons.

Our undertaking shows appreciable specificity, which will ensure that the chances of the result showing the positive

test for the patient having no disease are less. The sensitivity is found low, which can be enhanced by changing the threshold level settings. However, it will sacrifice specificity.

6. Conclusion

The method was developed for detecting exudates in retinal fundus images by performing morphological operations on the contrast limited adaptive histogram equalized green channel image. The optic disc detection and segregation is achieved based on circularity concept. The standard deviation of the optic disc removed image is used to find a cluster of exudates that are closely distributed, which helps to limit the effect of extreme values. The proposed technique reported highest accuracy of 99.13% and specificity of 99.15%. The undertaking is intended to serve the application like medical camps, where the large quantum of patient needs to be diagnosed quickly. Here, high specificity is demanded so that non-diseased people will be omitted fast. Further, only primarily suspected diseased cases can be examined thoroughly. The less computations in the morphological algorithm resulted in the low processing time.

In future work, the issue of low sensitivity can be addressed by upgrading the detection methods for the optic disc, blood vessels and locating the light and small exudates. The technique can also be developed to identify microaneurysms and haemorrhages in order to determine the severity degree of diabetic retinopathy.

References

1. World health organization :classification of diabetes mellitus ,2019.
2. Global report on diabetes. Geneva : World Health Organization, 2016.
3. IDF Diabetes Atlas. 8th Edition. Brussels : International Diabetes Federation, 2017
4. M. Niemeijer, B. van Ginneken, J. Staal, M. S. A. Suttorp-Schulten and M. D. Abramoff, "Automatic detection of red lesions in digital color fundus photographs," in IEEE Transactions on Medical Imaging, vol. 24, no. 5 : 584-592, 2005, doi: 10.1109/TMI.2005.843738.
5. Gardner, G G et al., "Automatic detection of diabetic retinopathy using an artificial neural network: a screening tool." The British journal of ophthalmology vol. 80,11: 940-4.1996 doi:10.1136/bjo.80.11.940
6. Neeti Gupta, Rohit Gupta, "Diabetic Retinopathy – An Update" JIMSA Jan. - Vol. 28 No. 1, 2015
7. King RC, Dobree JH, Kok D, Foulds WS, Dangerfield WG,"Exudative diabetic retinopathy. spontaneous changes and effects of a corn oil diet." Br J Ophthalmol.47(11):666-72. 1963,doi: 10.1136/bjo.47.11.666. PMID: 14211666; PMCID: PMC505868.
8. Hsu, Weihua&Pallawala, P. & Lee, Mong & Au Eong, Kah-Guan,"The role of domain knowledge in the detection of retinal hard exudates". Proceedings / CVPR, IEEE Computer Society Conference on Computer Vision and Pattern Recognition. IEEE Computer Society Conference on Computer Vision and Pattern Recognition. 2. II-246,2001,doi: 10.1109/CVPR.2001.990967
9. Sinthanayothin, C et al., "Automated localisation of the optic disc, fovea, and retinal blood vessels from digital colour fundus images." The British journal of ophthalmology vol. 83,8: 902-10, 1999,doi:10.1136/bjo.83.8.902
10. T. Walter, J. -. Klein, P. Massin and A. Erginay, "A contribution of image processing to the diagnosis of diabetic retinopathy-detection of exudates in color fundus images of the human retina," in IEEE Transactions on Medical Imaging, vol. 21, no. 10: 1236-1243, 2002, doi: 10.1109/TMI.2002.806290.
11. Osareh, A et al., "Automated identification of diabetic retinal exudates in digital colour images." The British journal of ophthalmology vol. 87,10: 1220-3, 2003. doi:10.1136/bjo.87.10.1220
12. Zhang, X., &Chutatape, O., "Detection and classification of bright lesions in color fundus images". 2004 *International Conference on Image Processing, ICIP '04., 1*, 139-142 Vol. 1, 2004.
13. Sopharak, Akara et al., "Automatic Exudate Detection from Non-dilated Diabetic Retinopathy Retinal Images Using Fuzzy C-means Clustering." Sensors (Basel, Switzerland) vol. 9,3: 2148-61, 2009. doi:10.3390/s90302148
14. Sánchez, Clara I et al., "A novel automatic image processing algorithm for detection of hard exudates based on retinal image analysis." Medical engineering & physics vol. 30,3: 350-7, 2008, doi:10.1016/j.medengphy.2007.04.010
15. M. PonniBala, S. Vijayachitra, "Computerised Retinal Image Analysis to Detect and Quantify Exudates Associated with Diabetic Retinopathy" International Journal of Computer Applications (0975 – 8887) Vol. 54,no.2, 2012.
16. H. F. Jaafar, A. K. Nandi and W. Al-Nuaimy, "Detection of exudates from digital fundus images using a regionbased segmentation technique," in Signal Processing Conf. 19th European Conf., EUSIPCO 2011, Barcelona,pp. 1020–1024, 2011.
17. U. Aftab and M. U. Akram, "Automated identification of exudates for detection of macular edema," 2012 Cairo International Biomedical Engineering Conference (CIBEC), , pp. 27-30, 2012, doi: 10.1109/CIBEC.2012.6473307.
18. M. K. Dutta et al., "Exudates detection in digital fundus image using edge based method & strategic thresholding," 38th International Conference on Telecommunications and Signal Processing (TSP), , pp. 748-752, 2015.doi: 10.1109/TSP.2015.7296364.
19. VesnaZeljkojic, Milena Bojic, Shengwei Zhao, Claude Tameze, VentzeslavValev, "Exudates and Optic Disc Detection in Retinal Images of Diabetic Patients" Concurrency and Computation Practice and Experience. 2015

20. A. Singh, N. Sengar, M. K. Dutta, K. Riha and J. Minar, "Automatic exudates detection in fundus image using intensity thresholding and morphology," 7th International Congress on Ultra Modern Telecommunications and Control Systems and Workshops (ICUMT), pp. 330-334, 2015. doi: 10.1109/ICUMT.2015.7382452.
21. Popescu, D., Ichim, L., & Caramihale, T., "Detection of exudates and hemorrhages using an efficient criterion for feature selection". *39th International Conference on Telecommunications and Signal Processing (TSP)*, 711-715, 2016.
22. F. Ghaffar, B. Uyyanonvara, C. Sinthanayothin, L. Ali and H. Kaneko, "Detection of exudates from retinal images using morphological compact tree," 13th International Joint Conference on Computer Science and Software Engineering (JCSSE), pp. 1-5, 2016 doi:10.1109/JCSSE.2016.7748858.
23. Win, K.Y., & Choomchuay, S., "Automated detection of exudates using histogram analysis for Digital Retinal Images". *International Symposium on Intelligent Signal Processing and Communication Systems (ISPACS)*, 1-6, 2016.
24. Long, Shengchun et al., "Automatic Detection of Hard Exudates in Color Retinal Images Using Dynamic Threshold and SVM Classification: Algorithm Development and Evaluation." *BioMedresearch international* vol. 2019 3926930, 2019, doi:10.1155/2019/3926930
25. WilverAuccahuasia , Edward Floresb , Fernando Sernaqueb , Juanita Cuevab , Monica DiazbElizabeth Oré., " Recognition of hard exudates using Deep Learning" *Procedia Computer Science* 167 2343–2353. ISSN 1877-0509, 2020
26. Muhammad Mateen, Junhao Wen, NasrullahNasrullah, Song Sun, Shaukat Hayat, "Exudate Detection for Diabetic Retinopathy Using Pretrained Convolutional Neural Networks" *complexity*, Volume 2020, Article ID 5801870, 11 pages, 2020, doi:10.1155/2020/5801870.
27. PrasannaPorwal, SamikshaPachade, RaviKamble, ManeshKokare, GirishDeshmukh, VivekSahasrabuddhe and FabriceMeriaudea , "Indian Diabetic Retinopathy Image Dataset (IDRiD): A Database for Diabetic Retinopathy Screening Research" *Dataset*: 10.21227/H25W98, Dataset License: CC-BY 4.0, Data 2018, 3, 25; doi:10.3390/data3030025, www.mdpi/journal/data
28. P.S. Vikhe, V.R. Thool, "A wavelet and adaptive threshold-based contrast enhancement of masses in mammograms for visual screening" *Int. J. Biomedical Engineering and Technology*, Vol. 30, No. 1, 2019.
29. Reza, A.M., "Realization of the Contrast Limited Adaptive Histogram Equalization (CLAHE) for Real-Time Image Enhancement". *The Journal of VLSI Signal Processing-Systems for Signal, Image, and Video Technology* **38**, 35–44, 2004. doi :10.1023/B:VLSI.0000028532.53893.82
30. MoscosoM., "Introduction to Image Reconstruction". In: Bonilla L.L. (eds) *Inverse Problems and Imaging. Lecture Notes in Mathematics*, vol 1943. Springer, Berlin, Heidelberg. https://doi.org/10.1007/978-3-540-78547-7_1
31. N. Otsu, "A Threshold Selection Method from Gray-Level Histograms," in *IEEE Transactions on Systems, Man, and Cybernetics*, vol. 9, no. 1, pp. 62-66, 1979, doi: 10.1109/TSMC.1979.4310076.
32. Sopharak, A., Uyyanonvara, B., & Barman, S., "Fine Exudate Detection using Morphological Reconstruction Enhancement." *International journal of applied biomedical engineering* vol.1, no.1 2010
33. K. Wisaeng and W. Sa-Ngiamvibool, "Exudates Detection Using Morphology Mean Shift Algorithm in Retinal Images," in *IEEE Access*, vol. 7, pp. 11946-11958, 2019, doi: 10.1109/ACCESS.2018.2890426.